

Single crystal structure of pure and Zn ion exchanged clinoptilolite: Comparison of low temperature and room temperature structures and Cu vs. Mo radiation

L. Dimova*, B. L. Shivachev, R. P. Nikolova

*Bulgarian Academy of Sciences, Institute of Mineralogy and Crystallography, 1113 Sofia,
Acad. Georgi Bonchev Str., Bl. 107, Bulgaria*

Received January 27, 2011; Revised April 12, 2011

Natural clinoptilolite crystals were Zn ion-exchanged. The crystals were initially Na-exchanged and then the precursor was treated with 1 M ZnCl₂ solution for three months at 383 K to obtain the Zn exchanged form. Chemical analyses with an EDS/SEM for Zn exchanged samples showed that the cation exchange is partial and that several other cations remained in the structure. Duplicate single crystal structure refinements were performed for both Natural and Zn-exchanged clinoptilolite samples for revealing the structural peculiarities. Most of the Zn atoms are not bonded to framework oxygen. The Zn cations are located in the center of the ten-membered channel forming a disordered [Zn(H₂O)₆] complexes.

Key words: clinoptilolite, Zn ion-exchange, single crystal structure.

INTRODUCTION

The naturally occurring Heulandite-type zeolites, including heulandite (Heu) and clinoptilolite (CPT) are the most abundant minerals on earth, exhibiting a zeolite structure. Large, easily accessible surface deposits mainly of volcanoclastic origin, allow clinoptilolite low cost production by simple excavation. Its applications [1] range from wastewater treatment, aquacultural and agricultural applications (fertilizer), as a deodorizer and up to Fluid Catalytic Cracking (FCC) [2]. Nowadays the focus is shifted onto its ion exchange properties and potential medical and pharmaceutical applications [3–5]. For a better understanding of clinoptilolite applications a pure material is required and for single-crystal X-ray experiments large crystals are demanded. Single crystal structural studies have the advantage over powder XRD, spectroscopic and NMR studies that multiple inclusion sites (cation, anion, water etc.) can directly be distinguished. However, natural clinoptilolite rocks are rather inhomogeneous and are obtained as mixtures of phases (e.g. other zeolites, SiO₂, feldspars, clays, Fe-oxides/hydroxides) thus the occurrence of individual large clinoptilolite crystals should be thoroughly exploited. Heulandite

and clinoptilolite are isotypic (space group C2/m, $a \approx 17.7$, $b \approx 17.9$, $c \approx 7.4$ Å, $\beta \approx 116^\circ$) [6]. Distinction between heulandite and clinoptilolite is done on the basis of the Si/Al ratio, silica-rich crystals (Si/Al > 4) are named clinoptilolites while aluminous ones (Si/Al < 4) are heulandites [7].

The crystal structure shows the existence of three types of structural channels confined by ten- and eight-membered tetrahedral ring systems (Fig. 1). From crystal-chemistry point of view aluminosilicate framework possesses a negative charge that is equilibrated by cations located in the channels (simplified formula: $[\text{Me}^+, \text{Me}^{2+}, \text{N}\times\text{H}_2\text{O}]^{6+} [\text{Al}_6\text{Si}_{30}\text{O}_{72}]^{6-}$). Detailed structural investigations on complete and partially ion exchanged on Na, K, Rb, Cs, Cd, Ag, Mn, Cu, Pb, Sr, Er, La clinoptilolite have been carried out [8–11] and summarizing the results some typical positions for cation placement in the channels have been assigned [6]. However, no detailed single crystal structural studies for Zn ion-exchanged clinoptilolite (ZnCPT) have been undertaken. The conducted by us studies revealed that CPT tolerates limited to complete Zn ion-exchange [12].

The aims of the present study are: (1) to obtain a Zn rich clinoptilolite via cation exchange; (2) to study the positioning and coordination of extra-framework Zn atoms by single-crystal X-ray methods; and (3) to compare the quality of the single-crystal data conducted under various conditions.

* To whom all correspondence should be sent:
E-mail: anien@abv.bg

EXPERIMENTAL

Ion-exchange

Clinoptilolite from Beli plast deposit, Kardzhali, Bulgaria, was used for this study. For three months a set of single crystals with average size between 0.2 and 0.08 mm was treated in an aqueous NaCl solution (1 M) in a Teflon reactor with temperature slowly oscillating in an oven around 383 K. The NaCl solution was replaced weekly. The NaCl exchange is an indirect method that avoids the use of an acid treatment for the preparation of H-CPT form. The obtained Na-exchanged form was subsequently Zn-exchanged under similar conditions (1 M aqueous ZnCl₂ solution for three months at 383, weekly exchange of the solution and with additional pH monitoring).

X-ray single crystal analyses

Crystal of CPT and ZnCPT with approximate dimension of 0.14×0.12×0.12 mm and 0.18×0.12×0.12 mm respectively was placed on a glass fiber and mounted on an Enraf-Nonius CAD-4 diffractometer and Oxford diffraction Supernova diffractometer equipped with Atlas CCD detector. X-ray data collection was carried out at 290 (CAD-4 and Supernova) and 120 K (Supernova) with monochromatized Mo-K α radiation ($\lambda = 0.71073 \text{ \AA}$) and Cu K α radiation ($\lambda = 1.54184 \text{ \AA}$). During the low temperature data collection the sample was kept at 120 K with an Oxford Instruments Cobra controller device and a nitrogen atmosphere. The unit cell parameters were determined using 15 reflections and refined employing 22 higher-angle reflections, $18 < \theta < 20^\circ$; the $\omega/2\theta$ technique was used for data collection using CAD-4 Nonius Diffractometer Control Software [13]. For the Supernova the data reduction and analysis for these structures were carried out with the CrysAlisPro program [14]. Lorentz and polarization corrections were applied to intensity data using the WinGX [15]. The structure was solved by direct methods using SHELXS-97 [16] and refined by full-matrix least-squares procedure on F^2 with SHELXL-97 [16].

Scanning electron microscopy (SEM), energy dispersive X-ray microanalysis (EDS)

The structure of the clinoptilolite crystals was examined with the SEM Jeol JSM-840A. Chemical composition and phase changes in CPT/ZnCPT were evaluated by EDS analysis in the Link AnalyticalAN10000 analyzer.

RESULTS AND DISCUSSION

The clinoptilolite (CPT and ZnCPT) chemical composition obtained from SEM/EDS data is given in Table 1.

The obtained chemical composition of the natural single crystals is close to the ideal balance between +/- charges in the CPT structure (+/- = 5.76/5.72 = extra framework cations). Following the ion exchange with NaCl and ZnCl (aggregate time of 6 months) the Si/Al ratio is only slightly altered compared to the initial one (5.31 vs. 5.16) thus one can presume that the CPT framework is intact. The results also clearly indicate that Zn ion-exchange has taken place. If we compare the charge of the extra framework cations for CPT (5.76) and ZnCPT (5.83) we can see that Na, Ca, K, Mg, Ba charge is slightly lower than expected in Zn exchanged sample: $(4.90 \text{ Na}_{0.89} \text{ Ca}_{1.40} \text{ K}_{0.07} \text{ Mg}_{0.11} \text{ Ba}_{0.46} + 0.66 \text{ Zn}) = 5.56$ (though one can argue that the result is comparable to the method error). Further, the amounts of K, Mg and Ba are almost identical in CPT and ZnCPT and as Na is a monovalent cation there is great probability that Zn \leftrightarrow Ca exchange has occurred. However, typical Ca and Zn ion coordination spheres are significantly different.

The CAD4 diffractometer Mo source is a fine focus sealed tube. The Supernova is equipped with Agilent micro-focus Mova (Mo radiation) and Nova (Cu radiation) sources. The Mova produces typically 2.5x more intense radiation flux than the Mo fine focus sealed tube while the Nova intensity is usually 3x that of the Mova.

Structure solution and refinement

As an example we are going to describe the solution of the natural CPT from Beliplast (CAD4, Mo

Table 1. Chemical composition of natural and Zn exchanged clinoptilolite

	Chemical formula	Si/Al	+/- charges
CPT	(Na _{0.35} Ca _{1.99} K _{0.09} Mg _{0.18} Ba _{0.49}) Al _{5.72} Si _{30.28} O ₇₂	5.31	5.76/5.72
ZnCPT	(Na _{0.89} Ca _{1.40} K _{0.07} Mg _{0.11} Ba _{0.46} Zn _{0.33}) Al _{5.83} Si _{30.17} O ₇₂	5.16	5.83/5.56

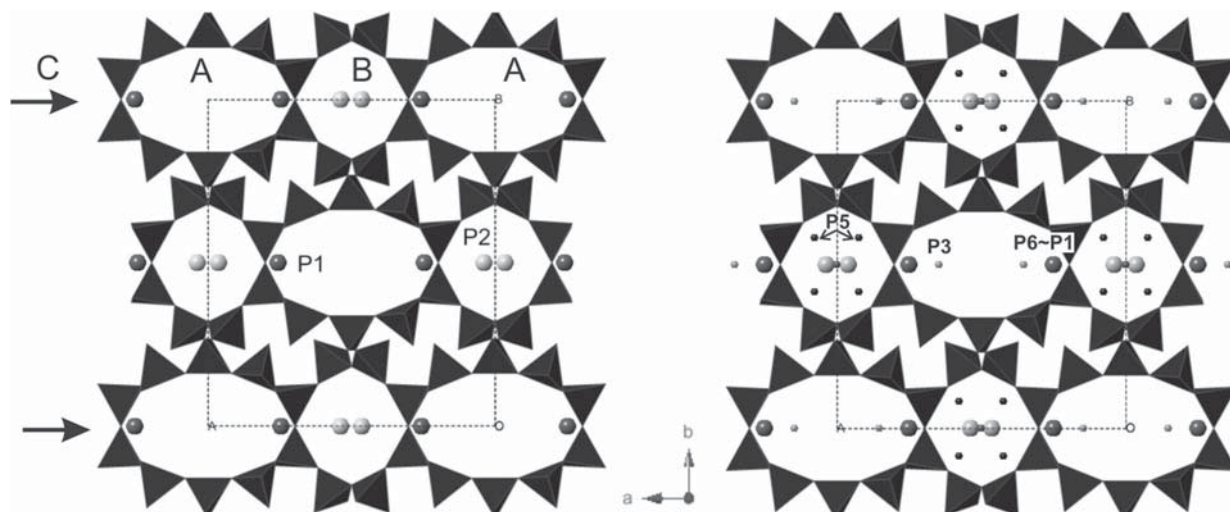


Fig. 1. Polyhedral model of a portion of the clinoptilolite structure projected parallel to the *c*-axis illustrating the porous structure: the ten-membered A and the eight-membered B channels are clearly visible in the projection while the eight-membered C channels, indicated by arrows, connect A and B channels in the *bc* plane. The locations of the most important extra-framework sites are also indicated.

wavelength). The “hkl” file was generated through XCAD4 as implemented in WinGX [15] and a direct methods solution using ShelX86 [16] was initiated. The resulting electron density clearly allowed the positioning of the framework atoms, Si, Al and O and in surplus located two extra framework positions (P1 and P2) with respective coordinates 0.242700, 0.0, 0.052000 and 0.461700, 0.0, 0.630300 (Fig. 1). At this stage the main statistical parameters look very promising: isotropic refinement, $R = 0.1496$, $R_w = 0.1878$, $wR = 0.4133$, $GOF = 2.221$. A subsequent cycles of refinement allowed the location of four electron density peaks (Q1=P3, Q2=P4, Q3=P5 and Q4=P6 with respective values of 9.16, 5.16, 4.81 and 3.15) located in the CPT channels which were clearly more pronounced than the other ones (the values of Q5 was 1.18). The P1 and P6 positions are too close to be occupied simultaneously $\sim 0.77 \text{ \AA}$ (“forbidden positions”) which is not uncommon case for CPT structures [7–9]. The resulting statistical parameters were $R = 0.1018$, $R_w = 0.1423$, $wR = 0.3286$, $GOF = 1.105$ (isotropic refinement), thus indicating that the model is very close to the collected data.

Now let’s look in details for each accounted location. P1 is located in the A channel and is at ~ 2.97 and 3.14 \AA from framework oxygen (Fig. 3). The position (P1) has been observed by Koyama and Takeuchi [17] and later on subsequent studies [11] have found that the position is occupied by “large” cations like potassium K. P2 is also known from literature [17] and the cation that is associated with this position is Ca (or Na). P3 is close to P1 and is

normally occupied by Na. P4 is positioned in the center of channel B (nearby P2) and is associated to coordination water (usually with occupancy around 1). P5, like P4 is located in B channel and is also reported as being coordination water. P6 is

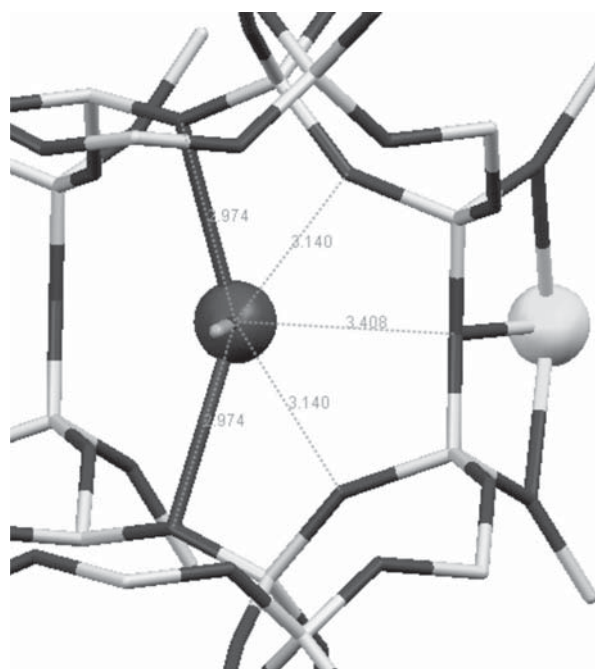


Fig. 2. P1 coordination sphere, P4 in orange, P2 in yellow, oxygen framework atoms in red and Si/Al in white. Reported contacts are in \AA .

close to P1 and is associated to Na or Ba or may be an artifact from the isotropical refinement.

Thus if we crosscheck with the calculated from EDS chemical formula where we have Na, Ca, K, Mg and Ba: K/Na/Ca = P1, Ca = P2, Na = P3, Ba = P6 (forbidden with P1), P4 and P5 water. The missing Mg, according to available structural data [17] is normally positioned in the center of A channel – not allocated at this stage of refinement

(or alternatively may occupy one of the observed positions P1 through P6, Figure 2).

After a few cycles of refinement an additional water position was detected. Further the occupancies of water molecules and cations were refined and finally the structure was refined anisotropically. The final refinement parameters are presented in Table 2. The same crystal was mounted on an Oxford Supernova diffractometer with ATLAS CCD and two datasets

Table 2. Crystal data

CPT-pure CAD4	CPT-pure Supernova Cu	CPT-pure Supernova Mo Low Temperature	CPT Zn exchanged CAD4 Mo radiation	CPT Zn exchanged Supernova Cu
Monoclinic, <i>C2/m</i>	Monoclinic, <i>C2/m</i>	Monoclinic, <i>C2/m</i>	Monoclinic, <i>C2/m</i>	Monoclinic, <i>C2/m</i>
Hall symbol: $-C\ 2y$	Hall symbol: $-C\ 2y$	Hall symbol: $-C\ 2y$	Hall symbol: $-C\ 2y$	Hall symbol: $-C\ 2y$
$a = 17.229\ (4)\ \text{\AA}$	$a = 17.2660\ (4)\ \text{\AA}$	$a = 17.2032\ (4)\ \text{\AA}$	$a = 17.259\ (2)\ \text{\AA}$	$a = 17.3081\ (16)\ \text{\AA}$
$b = 17.931\ (5)\ \text{\AA}$	$b = 17.9954\ (3)\ \text{\AA}$	$b = 17.9697\ (3)\ \text{\AA}$	$b = 17.955\ (2)\ \text{\AA}$	$b = 17.9896\ (11)\ \text{\AA}$
$c = 7.388\ (2)\ \text{\AA}$	$c = 7.39542\ (17)\ \text{\AA}$	$c = 7.3827\ (2)\ \text{\AA}$	$c = 7.3930\ (15)\ \text{\AA}$	$c = 7.4020\ (6)\ \text{\AA}$
$\beta = 113.66\ (3)^\circ$	$\beta = 113.731\ (3)^\circ$	$\beta = 113.717\ (3)^\circ$	$\beta = 113.70\ (2)^\circ$	$\beta = 113.705\ (11)^\circ$
$V = 2090.5\ (9)\ \text{\AA}^3$	$V = 2103.52\ (8)\ \text{\AA}^3$	$V = 2089.51\ (8)\ \text{\AA}^3$	$V = 2097.6\ (6)\ \text{\AA}^3$	$V = 2110.3\ (3)\ \text{\AA}^3$
$Z = 1$	$Z = 1$	$Z = 1$	$Z = 1$	$Z = 1$
$D_x = 2.189\ \text{Mg m}^{-3}$	$D_x = 2.169\ \text{Mg m}^{-3}$	$D_x = 2.179\ \text{Mg m}^{-3}$	$D_x = 2.184\ \text{Mg m}^{-3}$	$D_x = 2.189\ \text{Mg m}^{-3}$
Cell parameters from 22 reflections	Cell parameters from 10 frames	Cell parameters from 10 frames	Cell parameters from 22 reflections	Cell parameters from 10 frames
$\theta = 18\text{--}20^\circ$			$\theta = 16.3\text{--}17.7^\circ$	
Prism, colourless	Prism, colourless	Prism, colourless	Prism, colorless	Prism, colorless
$0.14 \times 0.12 \times 0.12\ \text{mm}$	$0.14 \times 0.12 \times 0.12\ \text{mm}$	$0.14 \times 0.12 \times 0.12\ \text{mm}$	$0.18 \times 0.12 \times 0.12\ \text{mm}$	$0.18 \times 0.12 \times 0.12\ \text{mm}$

Table 2. Data collection

Enraf Nonius CAD4	Oxford Supernova	Oxford Supernova	Enraf Nonius CAD4	Oxford Supernova
Radiation source: sealed tube	Radiation source: micro focus	Radiation source: micro focus	Radiation source: sealed tube	Radiation source: micro-focus
Mo $K\alpha$ radiation $\lambda = 0.71073\ \text{\AA}$	Cu $K\alpha$ radiation $\lambda = 1.54184\ \text{\AA}$	Mo $K\alpha$ radiation $\lambda = 0.71073\ \text{\AA}$	Mo $K\alpha$ radiation $\lambda = 0.71073\ \text{\AA}$	Cu $K\alpha$ radiation $\lambda = 1.54184\ \text{\AA}$
$T = 293(2)\ \text{K}$	$T = 293(2)\ \text{K}$	$T = 123(1)\ \text{K}$	$T = 293(2)\ \text{K}$	$T = 293(2)\ \text{K}$
4830 measured reflections	4344 measured reflections	11878 measured reflections	4767 measured reflections	4218 measured reflections
2569 independent reflections	2251 independent reflections	5427 independent reflections	2579 independent reflections	2109 independent reflections
1602 reflections with $I > 2\sigma(I)$	2192 reflections with $I > 2\sigma(I)$	4021 reflections with $I > 2\sigma(I)$	1695 reflections with $I > 2\sigma(I)$	2000 reflections with $I > 2\sigma(I)$
$R_{\text{int}} = 0.061$	$R_{\text{int}} = 0.048$	$R_{\text{int}} = 0.029$	$R_{\text{int}} = 0.086$	$R_{\text{int}} = 0.039$
$\theta_{\text{max}} = 28.0^\circ$	$\theta_{\text{max}} = 76.2^\circ$	$\theta_{\text{max}} = 37.7^\circ$	$\theta_{\text{max}} = 28.0^\circ$	$\theta_{\text{max}} = 76.2^\circ$
$\theta_{\text{min}} = 1.7^\circ$	$\theta_{\text{min}} = 3.7^\circ$	$\theta_{\text{min}} = 3.0^\circ$	$\theta_{\text{min}} = 1.7^\circ$	$\theta_{\text{min}} = 3.7^\circ$
$h = 0 \rightarrow 22$	$h = -21 \rightarrow 18$	$h = -29 \rightarrow 25$	$h = 0 \rightarrow 22$	$h = -17 \rightarrow 21$
$k = -23 \rightarrow 23$	$k = -14 \rightarrow 22$	$k = -28 \rightarrow 30$	$k = -23 \rightarrow 23$	$k = -22 \rightarrow 13$
$l = -9 \rightarrow 8$	$l = -8 \rightarrow 9$	$l = -12 \rightarrow 12$	$l = -9 \rightarrow 8$	$l = -9 \rightarrow 6$
3 standard reflections every 120 min	Dark frame: every 50 frames	Dark frame: every 50 frames	3 standard reflections every 120 min	Dark frame: every 50 frames
intensity decay: 0%	intensity decay: 0%	intensity decay: 0%	intensity decay: 1%	intensity decay: 0%

with Mo and Cu radiation were collected. The structure solution and refinement was conducted according to the above mentioned procedure and the final refinement parameters are shown in Table 2.

Zinc exchanged CPT structure solution

Using the results from SEM/EDS the main peculiarities in the CPT vs. ZnCPT composition

Table 2. Refinement

Refinement on F^2	Refinement on F^2	Refinement on F^2	Refinement on F^2	Refinement on F^2
Least-squares matrix: full	Least-squares matrix: full	Least-squares matrix: full	Least-squares matrix: full	Least-squares matrix: full
$R[F^2 > 2\sigma(F^2)] = 0.074$	$R[F^2 > 2\sigma(F^2)] = 0.072$	$R[F^2 > 2\sigma(F^2)] = 0.067$	$R[F^2 > 2\sigma(F^2)] = 0.077$	$R[F^2 > 2\sigma(F^2)] = 0.072$
$wR(F^2) = 0.238$	$wR(F^2) = 0.241$	$wR(F^2) = 0.233$	$wR(F^2) = 0.277$	$wR(F^2) = 0.218$
$S = 0.94$	$S = 1.06$	$S = 0.74$	$S = 0.98$	$S = 1.12$
2569 reflections	2251 reflections	5427 reflections	2579 reflections	2109 reflections
173 parameters	173 parameters	161 parameters	162 parameters	177 parameters
0 constraints	0 constraints	0 constraints	0 constraints	0 constraints
$w = 1/[\sigma^2(F_o^2) + (0.1579P)^2 + 2.2394P]$ where $P = (F_o^2 + 2F_c^2)/3$	$w = 1/[\sigma^2(F_o^2) + (0.1147P)^2 + 37.7576P]$ where $P = (F_o^2 + 2F_c^2)/3$	$w = 1/[\sigma^2(F_o^2) + (0.1938P)^2 + 34.2667P]$ where $P = (F_o^2 + 2F_c^2)/3$	$w = 1/[\sigma^2(F_o^2) + (0.2P)^2]$ where $P = (F_o^2 + 2F_c^2)/3$	$w = 1/[\sigma^2(F_o^2) + (0.1147P)^2 + 37.7576P]$ where $P = (F_o^2 + 2F_c^2)/3$
$(\Delta/\sigma)_{\max} = 1.716$	$(\Delta/\sigma)_{\max} = 14.1$	$(\Delta/\sigma)_{\max} = 15$	$(\Delta/\sigma)_{\max} = 0.121$	$(\Delta/\sigma)_{\max} = 2.511$
$\Delta\rho_{\max} = 0.84 \text{ e } \text{\AA}^{-3}$	$\Delta\rho_{\max} = 0.68 \text{ e } \text{\AA}^{-3}$	$\Delta\rho_{\max} = 0.57 \text{ e } \text{\AA}^{-3}$	$\Delta\rho_{\max} = 0.89 \text{ e } \text{\AA}^{-3}$	$\Delta\rho_{\max} = 0.88 \text{ e } \text{\AA}^{-3}$
$\Delta\rho_{\min} = -0.90 \text{ e } \text{\AA}^{-3}$	$\Delta\rho_{\min} = -0.62 \text{ e } \text{\AA}^{-3}$	$\Delta\rho_{\min} = -0.83 \text{ e } \text{\AA}^{-3}$	$\Delta\rho_{\min} = -0.90 \text{ e } \text{\AA}^{-3}$	$\Delta\rho_{\min} = -0.93 \text{ e } \text{\AA}^{-3}$
Primary atom site location: structure-invariant direct methods, Secondary atom site location: difference Fourier map Absorption correction: none Extinction correction: none				

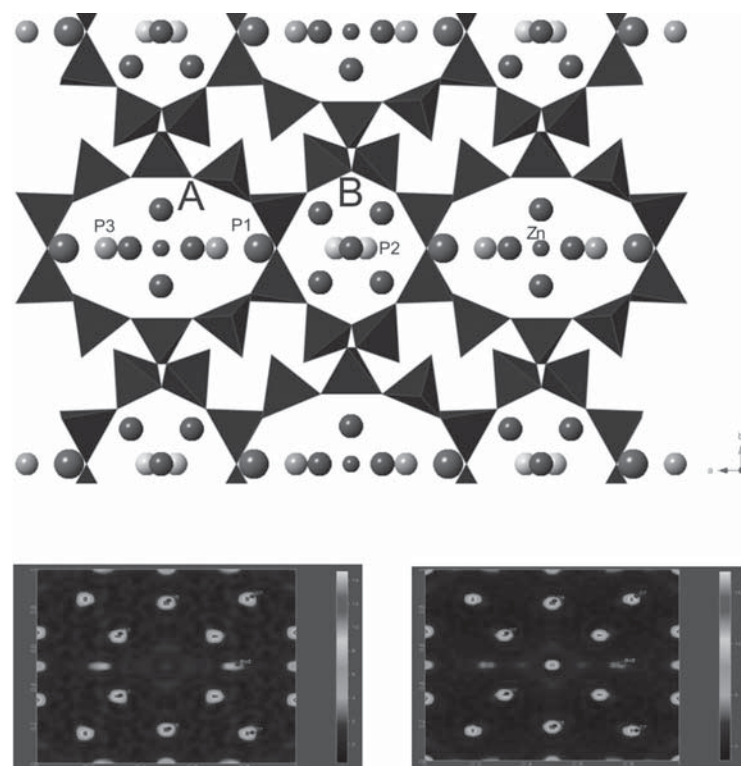


Fig. 3. Top: Polyhedral model of a portion of the ZnCPT structure (projected along ab plane) illustrating the porous structure: the ten-membered A and the eight-membered B channels are clearly visible in the projection. The locations of the most important extra-framework sites are also indicated. The Zn atom is located in the center of the A channel. Bottom: Fourier (Fobs) maps for natural clinoptilolite Mo radiation, CAD4 (left) and ZnCPT, Cu radiation, Supernova (right). The white arrow shows the absence/presence of electron density in CPT and ZnCPT.

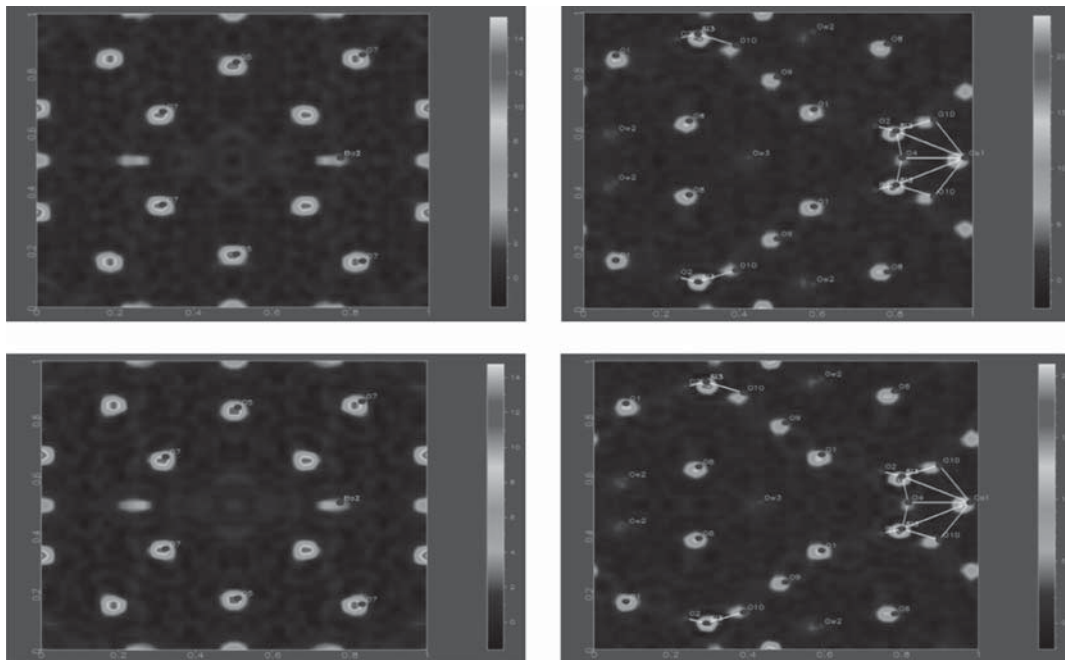


Fig. 4. Fourier maps (*ab* plane) of pure (top) and Zn exchanged (bottom) from CAD4 experiments Mo radiation.

are: Potassium and Barium values do not change only a reduction of Ca and Mg is observed (from ~ 2.00 to ~ 1.40 and ~ 0.18 to ~ 0.11 respectively). Thus a charge compensation of ~ 0.7 should be expected. Actually the results show that Na increases from ~ 0.4 to ~ 0.9 and some Zn (0.33) is

also present. The compensation is approximately equal (and taking into account the Si/Al variation – or the framework charge the result is indeed very good). Thus for the structure refinement two possibilities exist (this of course is an oversimplification): the Zn replaces Ca and Mg or

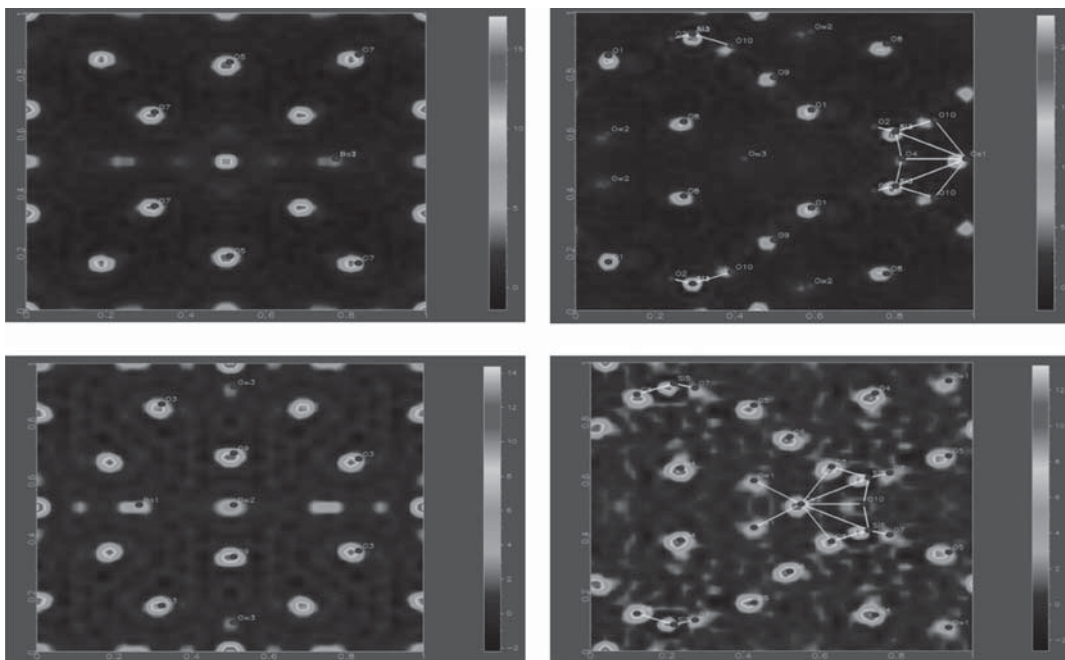


Fig. 5. Fourier maps (*ab* plane) of Zn exchanged low temperature Mo radiation (top) and Cu radiation (bottom) from Supernova experiments.

Zn is located in a different position (not observed in the structure of the pure CPT).

The crystal solution is performed as described previously and the statistics are shown in Table. 2.

The difference Fourier map clearly shows that the Zn cation occupies a new position (0 0.5 0) (Fig. 3), not observed in the natural CPT of Beli plast.

We do have 2 experiments on the CAD-4 and 3 on the Supernova (for pure and ion exchanged clinoptilolite). As expected the unit cell is monoclinic ($C2/m$) and the unit cell parameters do not change a lot from experiment to experiment and remain close to those of pure CPT. The framework atoms Si/Al and O are easily discernable in all experiments.

The difference Fourier map of pure and Zn exchanged CPT obtained from CAD4 experiments are comparable (Fig. 4). This is actually expected as the chemical variation for the whole crystal is ~2% and thus should not influence greatly data collection and refinement results. However, the difference Fourier densities maps clearly show that the more intense Cu radiation allows better positioning of the cations in the channels (Fig. 5).

CONCLUSIONS

It is visible that the experiments performed on the CAD4 (pure and ion exchanged) produce almost identical statistics as those on Oxford Supernova (CCD, Cu or Mo radiation). One may presume that pure and ion exchanged structures should be sufficiently “changed” in order to account for notable differences. On the other hand the differences are more pronounced for low temperature experiments and further more with the increase of radiation intensity e.g. Cu radiation. Thus, for accounting subtle structural variations low temperature and more intensive radiation are recommended.

Acknowledgments: The authors are grateful for the financial support of the Bulgarian National Science Fund through contract DRNF 02/1.

REFERENCES

1. H. G. K. M. Stöcker, J.C. Jansen, J. Weitkamp, *Advanced Zeolite Science and Applications*; (in Stud. Surf. Sci. Catal., vol. 85), Elsevier: Amsterdam, 1994; Vol. 85.
2. J. Mikulec; M. Vrbova. *Clean Technol Envir*, **10**, 121 (2008).
3. G. Cerri; M. de' Gennaro; M. C. Bonferoni; C. Caramella. *Appl Clay Sci*, **27**, 141 (2004).
4. V. J. Inglezakis; M. Stylianou; M. Loizidou. *J. Phys. Chem. Solids*, **71**, 279 (2010).
5. Y. Yukselen-Aksoy. *Appl. Clay Sci.*, **50**, 130 (2010).
6. A. Godelitsas; T. Armbruster. *Micropor. Mesopor. Mat.*, **61**, 3 (2003).
7. D. S. Coombs; A. Alberti; T. Armbruster; G. Artioli; C. Colella; E. Galli; J. D. Grice; F. Liebau; J. A. Mandarino; H. Minato; E. H. Nickel; E. Passaglia; D. R. Peacor; S. Quartieri; R. Rinaldi; M. Ross; R. A. Sheppard; E. Tillmanns; G. Vezzalini. *Canadian Mineralogist*, **35**, 1571 (1997).
8. J. Stolz; P. Yang; T. Armbruster. *Micropor. Mesopor. Mat.*, **37**, 233 (2000).
9. M. E. Gunter; T. Armbruster; T. Kohler; C. R. Knowles. *Am. Mineral.*, **79**, 675 (1994).
10. P. Yang; J. Stolz; T. Armbruster; M. E. Gunter. *Am. Mineral.*, **82**, 517 (1997).
11. T. Armbruster; P. Simoncic; N. Dobelin; A. Malsy; P. Yang. *Micropor. Mesopor. Mat.*, **57**, 121 (2003).
12. L. Dimova, PhD Thesis, IMC-BAS, 2011.
13. J. C. Schoone; Duisenbe.Aj. *Acta Crystallogr. A*, **25**, S81 (1969).
14. *Oxford Diffraction (2010). CrysAlis PRO. Oxford Diffraction Ltd, Yarnton, England.*
15. L. Farrugia. *Journal of Applied Crystallography*, **32**, 837 (1999).
16. G. M. Sheldrick. *Acta Crystallogr. A*, **64**, 112 (2008).
17. K. Koyama; Y. Takeuchi. *Z. Krist.*, **145**, 216 (1977).

МОНОКРИСТАЛНА СТРУКТУРА НА ПРИРОДЕН И ЦИНКОВО ЙОНООБМЕНЕН
КЛИНОПТИЛОЛИТ: СРАВНЕНИЕ НА СТРУКТУРНИТЕ РЕЗУЛТАТИ
ПРИ НИСКА И СТАЙНА ТЕМПЕРАТУРА, МЕДНО И МОЛИБДЕНОВО ЛЪЧЕНИЕ

Л. Димова*, Б. Л. Шивачев, Р. П. Николова

*Институт по минералогия и кристалография „Акад. Иван Костов“, Българска Академия на Науките,
ул. Акад. Г. Бончев бл. 107, 1113 София*

Постъпила на 27 януари, 2011 г.; приета на 12 април, 2011 г.

(Резюме)

Осъществен бе цинков йонообмен на монокристали на природен клиноптилолит. За получаване на цинкова форма първоначално бе приготвена натриева форма на образците. След това натриевите образци (форма) бяха третираны в продължение на три месеца с 1 М разтвор на $ZnCl_2$ при 383 К. Химическият анализ (енергийно дисперсионна спектроскопия) на цинковите образци показва частичен цинков йонообмен. Уточнена бе структурата на природния и цинково обменения клиноптилолит за изясняване на структурните промени. Повечето цинкови атоми не взаимодействат със скелетните кислородни атоми, а са разположени в центъра на десетчленния канал образувайки неподредени $[Zn(H_2O)_6]$ комплекси.